ESTIMATING PLANAR STRUCTURE IN SINGLE IMAGES BY LEARNING FROM EXAMPLES

Osian Haines and Andrew Calway
University of Bristol, UK
{*haines, andrew*}*@cs.bris.ac.uk*

Keywords: Monocular Vision: Image Understanding: Single Image: Plane Detection: Planar Structure: Scene Analysis: Learning: Nearest Neighbour: Topic Discovery: Latent Semantic Analysis: Spatiogram.

Abstract: Outdoor urban scenes typically contain many planar surfaces, which are useful for tasks such as scene reconstruction, object recognition, and navigation, especially when only a single image is available. In such situations the lack of 3D information makes finding planes difficult; but motivated by how humans use their prior knowledge to interpret new scenes with ease, we develop a method which learns from a set of training examples, in order to identify planar image regions and estimate their orientation. Because it does not rely explicitly on rectangular structures or the assumption of a 'Manhattan world', our method can generalise to a variety of outdoor environments. From only one image, our method reliably distinguishes planes from non-planes, and estimates their orientation accurately; this is fast and efficient, with application to a real-time system in mind.

1 INTRODUCTION

We address the problem of detecting planes in a single image, and estimating their 3D orientation. Man-made environments tend to contain many planes, and these can be used for compact representation of 3D scenes (Bartoli, 2007) and more efficient robot navigation (Gee et al., 2008; Martínez-Carranza and Calway, 2010). The ability to discover planes from only a single image would be beneficial in tasks including image understanding (Saxena et al., 2008), reconstructing 3D models (Košecká and Zhang, 2005) or wide baseline matching (Mičušík et al., 2008).

Finding planes in single images is challenging, due to the of lack of depth information. One popular approach is to use vanishing lines (Košecká and Zhang, 2005) to infer the scene geometry; however, this presupposes that such structure exists. Our approach (figure 1) is instead motivated by humans' apparent ability to understand scenes from one view: we learn from the appearance of a set of examples, manually labelled with their class and orientation; and describe these with feature descriptors in a bag of words, enhanced with spatial information. Using these training images allows us to identify image regions as planar – for building façades, stone walls and so on – or as non-planar – for foliage, vehicles, etc; then for planar regions we estimate their 3D orientation.

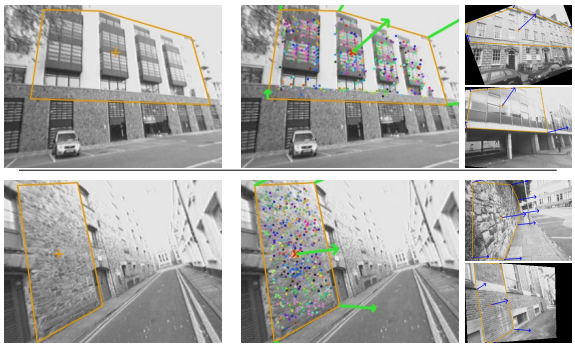

Figure 1: For a given image region (left) our algorithm classifies them as planes and estimates their orientation (centre) by finding training examples with similar orientation (right).

The method accurately separates planes from non-planes, making a sufficiently confident decision in 91% of cases, with 90% accuracy; plane orientation is predicted with a mean error of around 14° . Since we do not rely on vanishing lines or rectangular structure, the method is applicable to a wider range of scenes. The method is fast, able to make a decision for a new region in under one second. In this work we consider only the classification and orientation of individual image regions – automatic detection or segmentation is left for future work.

The paper is organised as follows. Section 2 dis-

cusses related work, then section 3 describes the details of the method. The results in section 4 show that the method can distinguish planes from non-planes and reliably predict their orientation in a variety of situations, and we conclude in section 5 with suggestions for future work.

2 RELATED WORK

A standard way to obtain geometry from a single image is the use of vanishing points – for example Košecká and Zhang (2005) rely on the orthogonality of planes to group lines and hypothesise rectangles, from which the pose of the camera can be recovered. Similarly, Mičušík et al. (2008) treat rectangle detection as a labelling problem, and use the detected planes' orientation for wide baseline matching.

Another cue which may be exploited is the distinctive appearance of certain parts of images. The method most similar to our own is that of Hoiem et al. (2007), which classifies 'super-pixels' into geometric classes, with orientations limited to being either horizontal, left, right, or front facing. A variety of features are used to create a coherent grouping from the initial super-pixels, resulting in an esimate of scene layout which has been used to create simple 3D models and for object recognition.

Saxena et al. (2008) focus on the related task of estimating depth, by training on range data from a laser scanner. From absolute and relative depth estimates at individual regions, a Markov Random Field is used to find a consistent depth map over the whole image. This has been used for sophisticated 3D model building, and to drive a high-speed toy car (Michels et al., 2005).

These methods show considerable progress in understanding single images; however they either rely on a restrictive 'Manhattan' assumption, or when applicable to more general scenes, can only obtain very coarse orientation or depth.

3 METHOD

Here we give an overview of our method, with more details in subsequent subsections. First, we gather a database of training examples, and manually assign a class (plane or not plane) and orientation (normal vector). Then the class and orientation of new regions are estimated using a K-Nearest Neighbour classifier, with similarity between regions evaluated as follows.

We use histograms of oriented gradients to describe the local appearance at salient points in an image region; since these are not informative enough on their own, we accumulate information using a bag of words approach, applying a variant of Latent Semantic Analysis (Deerwester et al., 1990) for dimensionality reduction.

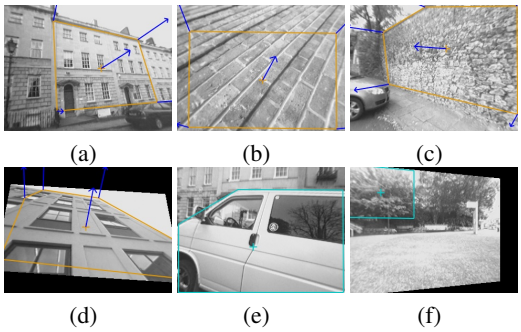

Figure 2: Examples of the training data we use, showing the manually selected region of interest and plane orientation (regions (a)-(d)); examples (d) and (f) were obtained by warping the original images.

The resulting vectors of latent 'topics' can be used for classification and orientation, but performance is improved by also considering their spatial configuration, which we represent using a histogram augmented with means and covariances – a 'spatiogram' (Birchfield and Rangarajan, 2005); as far as we are aware, using a spatiogram with a bag of words is novel. Further technical details can be found in (Haines and Calway, 2011).

3.1 Training Data

We collect training images of planes and non-planes from a variety of outdoor locations; these have a resolution of 320×240 pixels, and have been corrected for radial distortion. For each image we mark a region of interest, and assign them to the plane or non-plane class as appropriate. To get the true orientation, corners of a quadrilateral are marked, corresponding to a real rectangle; this defines two orthogonal sets of parallel lines, whose intersections define vanishing points $\mathbf{v}_1$ and $\mathbf{v}_2$. From this we calculate $\mathbf{n}$, the normal vector of the plane, using $\mathbf{n} = \mathbf{K}^{\mathrm{T}}\mathbf{l}$, where $\mathbf{l} = \mathbf{v}_1 \times \mathbf{v}_2$ is the vanshing line of the plane and $\mathbf{K}$ is the 3×3 matrix encoding the camera paramters (see figure 2).

We generate more training examples, to approximate planes seen from different viewpoints, by applying geometric transformations to the images. The simplest of these is to reflect about the vertical axis; we can also use the known relative pose of the planar regions to render new views from different locations, via the homography $\mathbf{H} = \mathbf{R} + \mathbf{t}\mathbf{n}^{\mathrm{T}}/d$, where $\mathbf{R}$ and $\mathbf{t}$ are the rotation matrix and translation vector for the new view, and d is the perpendicular distance to the

plane (defined up to scale). **H** is used to warp the image, to approximate the plane as seen from the new viewpoint, while the normal vector is rotated by **R**. In practice, the range of possible warps is limited by the image resolution.

3.2 Features

Following more typical object recognition approaches, we use descriptors that describe local orientations, in a histogram of oriented gradients. While this is the basis descriptors like SIFT (Lowe, 2004), we emphasise that our task is quite different: one of the benefits of SIFT is that it is invariant to a wide range of deformations, whereas our aim is specifically to determine plane orientation, not identity.

For each patch, we create gradient histograms for each quadrant, each with 12 angular bins, and concatenate these to form a descriptor of 48 dimensions – this is to capture some local structure information and build a richer descriptor.

Feature descriptors are created at salient points in the image, detected using the Difference of Gaussians detector (DoG), which gives a location and scale for each point. We use the scale to set the width of the patch to create the descriptor; scale selection seems to be advantageous since it ensures the most appropriate scale is being used at each location – this is verified by our results (see section 4), which show that multi-scale DoG detection is consistently superior to both single-scale DoG and FAST (Rosten and Drummond, 2006).

3.3 Bag of Words

The gradient descriptors capture information about local areas, but are not sufficient to disambiguate the structure of the scene, so we accumulate information over the whole region using the bag of words model. Each image region is represented by a histogram $\mathbf{x}$ over N words (typically $N = 300$; see section 4); term frequency - inverse document frequency weighting is used to down-weight common words, resulting in the weighted word vector $\mathbf{x}'$.

The words are found by quantising each of the D descriptor vectors $\mathbf{d}_d$ in the image region to a codebook; the codebook is built by clustering descriptors extracted from a set of typical images, using K-means with N cluster centres.

3.3.1 Topic Discovery

When N is large, the word vector will be high dimensional and sparse, and encodes no relationship bewteen potentially synonymous words. We overcome this using Orthogonal Nonnegative Matrix Factorisation (ONMF) to reduce the word histogram to a vector of latent topic weights. ONMF is related to Latent Semantic Analysis (LSA) (Deerwester et al., 1990), but differs in that the topic vectors have non-negative components (this is essential, see section 3.4).

ONMF factorises the term-document matrix $\mathbf{X}$ (where $\mathbf{X}_{nj}$ is the (weighted) number of occurrences of word n in image j, for M images) into $\mathbf{X} \approx \mathbf{WH}$, where $\mathbf{W}$ is the basis of the latent topic space (of rank T, the number of topics), and $\mathbf{H}$ contains the topic vectors. Word vectors are approximated by $\mathbf{x}'_i \approx \mathbf{W}\mathbf{h}_i$, where $\mathbf{h}_i$ is topic vector; conversely the topic vector for a new word vector is $\mathbf{h}_i = \mathbf{W}^{\mathrm{T}}\mathbf{x}_i$ (because $\mathbf{W}$ is orthogonal).

ONMF factorisation has no closed form solution, so we use an iterative method (Choi, 2008) which alternates the following updates (the columns of $\mathbf{W}$ must be re-normalised after each iteration):

$$\mathbf{W}_{nt} \longleftarrow \mathbf{W}_{nt} \frac{(\mathbf{X}\mathbf{H}^{\mathrm{T}})_{nt}}{(\mathbf{W}\mathbf{H}\mathbf{X}^{\mathrm{T}}\mathbf{W})_{nt}} \tag{1}$$

$$\mathbf{H}_{tm} \longleftarrow \mathbf{H}_{tm} \frac{(\mathbf{W}^{\mathrm{T}}\mathbf{X})_{tm}}{(\mathbf{W}^{\mathrm{T}}\mathbf{W}\mathbf{H})_{tm}} \tag{2}$$

3.4 Spatiograms

The constellation and star models (Fergus et al., 2005) have shown that representing the spatial arrangement of descriptors can improve performance; however because these are computationally expensive we use spatiograms instead (Birchfield and Rangarajan, 2005). A spatiogram is a higher-order generalisation of a histogram, where each bin also has a mean and covariance matrix, summarising the points contributing to it. A spatiogram $\mathbf{S}^{\mathsf{word}}$ over the words consists of a set of N triplets $s_n = \langle h_n, \mu_n, \Sigma_n \rangle$, were h_n is the bin count, μ_n is the mean and Σ_n the covariance matrix of the 2D coordinates for points contributing to the histogram bin. These are calculated as follows (altered so that we can use them for words, weighted words, or topics):

$$\mu_n = \frac{1}{\alpha} \sum_{d=1}^{D} \mathbf{v}_d \lambda_{dn} \tag{3}$$

$$\Sigma_n = \frac{\alpha}{\alpha^2 - \beta} \sum_{d=1}^{D} (\mathbf{v}_d - \mu_n)(\mathbf{v}_d - \mu_n)^{\mathrm{T}} \lambda_{dn} \tag{4}$$

where $\mathbf{v}_d$ is the 2D point at which descriptor $\mathbf{d}_d$ is created, and $\alpha = \sum_{d=1}^{D} \lambda_{dn}$, $\beta = \sum_{d=1}^{D} \lambda_{dn}^2$. For the basic word spatiogram, the element weight λ_{dn} is equal to 1 iff descriptor d quantises to word n; for the spatiogram of weighted words $\mathbf{S}^{\mathsf{word}\prime}$, $\lambda_{dn} = \frac{x'_n}{x_n}$,

i.e. the weighted occurrence of each word in the image. The topic spatiogram $\mathbf{S}^{\text{topic}}$ (of length T) uses $\lambda_{dt} = \frac{x'_n}{x_n}\mathbf{W}_{nt}$, where n is the word to which descriptor $\mathbf{d}_d$ quantises, and $\mathbf{W}_{nt}$ is the component of the basis vector for topic t relating to word n. Note that all weights must be positive – the reason we use ONMF instead of LSA. To compare spatiograms during classification we use the distance metric proposed by Ó Conaire et al. (2007). As we show in section 4, including spatial information boosts performance considerably.

3.5 Classification

To classify image regions and estimate their orientation, we use the relatively simple K-Nearest Neighbour classifier (KNN), chosen because analysing the chosen neighbours (see figures 1, 5) allows us to verify the method works as expected. Classification and orientation estimation can be performed simultaneously, by finding the K nearest neighbours: the class is assigned to the majority class of these, and the orientation is the mean of the 3D normal vectors. The proportion of neighbours in the larger class can be used as a confidence value to reject less certain classifications.

4 RESULTS

We collected an initial data set of 556 regions, from an urban area. For evaluation we use five-fold cross validation, and all tests use a value of $K = 5$ nearest neighbours, chosen for its superior performance (experiments omitted for brevity). First we analyse the performance of using ONMF and spatiograms, compared to the basic bag of words: we ran the algorithm using the (weighted) word histograms $\mathbf{x}'$ only, on word-spatiograms $\mathbf{S}^{\text{word}\prime}$, on topic vectors $\mathbf{h}$ only, and on topic spatiograms $\mathbf{S}^{\text{topic}}$ (the full method), for varying vocabulary size. Figure 3 shows results for classification accuracy and orientation error: in general, using topic discovery out-performs using words directly. Performance using word histograms decreases as they become sparser with increasing vocabulary size, but topic vectors can extract meaningful information from high dimensional word vectors, and performance remains almost constant. The graphs also clearly show the benefit of using spatiograms, which outperform histograms in all cases.

Interestingly, the results suggest that a very small number of words can be used without topic discovery – however, this constrains the method to use only small vocabularies, while are likely to generalise

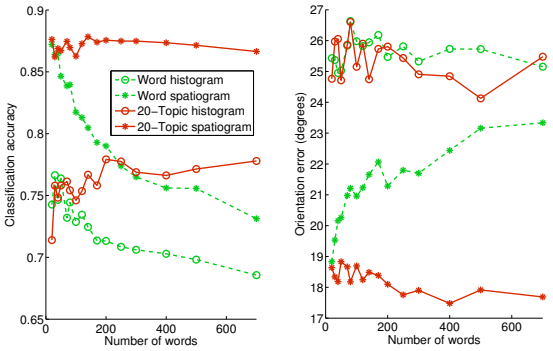

(a) Classification accuracy (b) Orientation error

Figure 3: Comparison of words and topics for different vocabulary sizes.

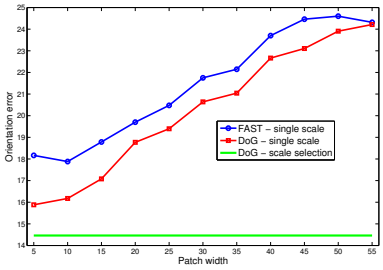

Figure 4: Using the Difference of Gaussians detector to choose the scale at which descriptors are built outperforms any single fixed scale, detected with either DoG or FAST.

poorly to new data sets. We verified this on our independent data set (see below) and found that in this case, using words alone gave an orientation accuracy of 20.5° (with standard deviation 18.1°), compared to using topics with error of 17.5° (std 15.9°).

We also ran an experiment to verify that using scale selection for the features is important. To ensure that no one scale was the best with scale selection simply choosing this occasionally, we tested scale selection (using the DoG detector) against fixed patch sizes with widths from 5 to 55, detected with both FAST and DoG; as figure 4 shows, scale selection is always better than any one scale.

Finally, we augment the training set by reflecting and warping regions (section 3.1), giving a total of 7752 (we do not test on the warped images, and ensure no region can match to a warped version of itself). This decreases the mean orientation error from 17.2° (standard deviation 13.7°) to 14.3° (std 12.9°).

For the remaining tests we use DoG for feature position and scale selection, the full set of warped examples, topic spatiograms in a vocabulary of 300 words, and we discard regions with a confidence below 0.7. The results we obtain for this situation is a recall (per-

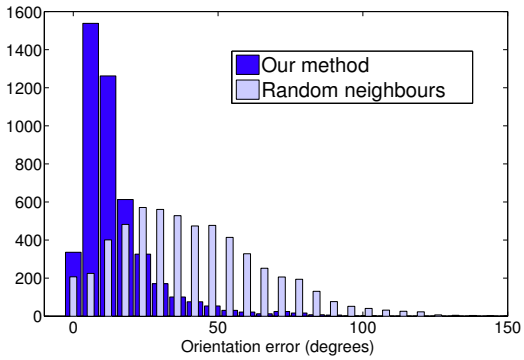

Figure 6: Distribution of errors for our method (dark), showing the majority of errors are small. Comparison to random neighbours method is superimposed (light).

centage of regions above the confidence threshold) of 91%, classification accuracy of 90%, and a mean orientation error of 14°. Figure 6 shows a histogram for orientation estimation, clearly showing that for the majority of regions (81%), the error is in the region of 0° to 20°. For comparison, and to indicate what a mean error of 14° signifies, we show resuts of an experiment using randomly chosen neighbours (histogram overlayed on the same plot). Clearly our method performs much better than chance – where the mean error is above 40°; this is a useful validation of the method, as it shows our method is not merely exploiting an artefact of how the data are distributed.

4.1 Independent Data

We also tested the algorithm on an independent data set collected from a different urban area, with the data set from above used for training. We achieved similar performance – a recall of 91%, classification accuracy of 87%, and mean orientation error of 17.5°. This set included some difficult regions – some without the classic rectangular-structure appearance (figures 1,7(d)), as well as images of pavements and roads, while we were careful to include *no* images of the ground in the training set, to test generalisation (figures 5 bottom, 7(f),7(g)). Figure 5 shows some example results of orientation estimation, alongside their nearest neighbours: these are often quite different in appearance, yet have a similar orientation. Figure 7 shows further examples, including non-planar regions. In these images, blue (thin) arrows indicate ground truth, and green (thicker) arrows are the estimated normal, with cyan circles denoting non-planar classification.

Figure 8 shows cases where the method performs poorly, for example 8(a) and 8(b) where all the neighbouring planes have very different orientation, a rare situation which requires further investigation. Figure 8(d) is a more difficult example, since it is quite different from any training images. Figure 8(e) may be confused by the railings, vertical trees and strong horizon line; and it is interesting to note that 8(f) is incorrectly determined to be a plane, when the side of a van could arguably be considered planar.

5 CONCLUSIONS

We have shown that we can reliably determine whether regions of images are planar or not, and estimate their orientation with respect to the viewpoint. This is successfully achieved using information from just one image in a bag of words representation, where performance is improved by using latent topic discovery and encoding spatial information. A KNN classifier was sufficient to demonstrate that the algorithm is able to classify a wide variety of plane and non-plane images and accurately estimate plane orientation (more advanced classifiers would be a natural aventue of future work); our method can work even in examples devoid of typical structure such as vanishing points and images of rectangles, and generalises well to new data. Now that we have shown this is possible, we intend to develop our algorithm to automatically segment planar regions from images – since we operate on whole regions as opposed to using local colour or edge information this will require a different approach to standard image segmentation.

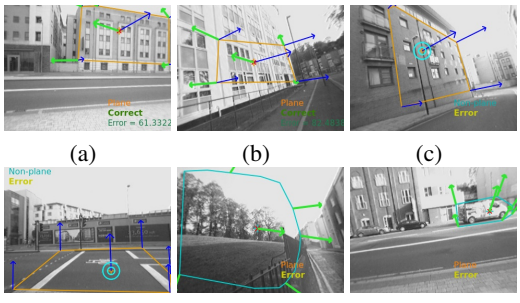

(a) (b) (c)

(d) (e) (f)

Figure 8: Where the method fails: (a),(b) show planes with incorrect orientation estimate, whereas (c),(d) are false negatives and (e),(f) are false positives for plane classification.

ACKNOWLEDGEMENTS

This work was funded by UK EPSRC. With thanks to José Martínez-Carranza and Sion Hannuna for useful discussions and advice.

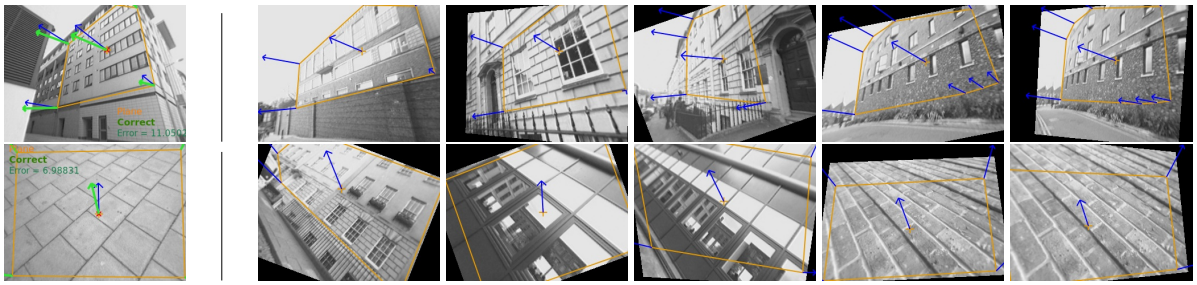

Figure 5: Examples of test planes (far left) and their 5 nearest neighbours. Top: matching to neighbours with different appearance. Bottom: accurate orientation estimation, though there are no images of the ground in the training set.

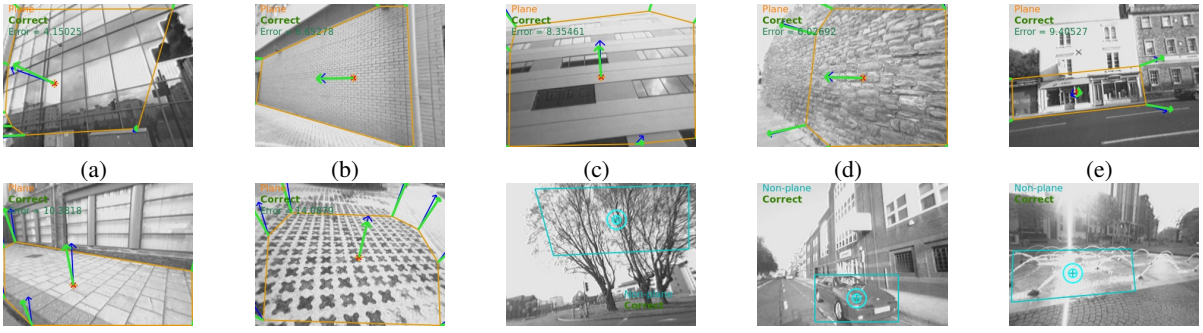

(a) (b) (c) (d) (e)

(f) (g) (h) (i) (j)

Figure 7: Examples of (a)-(g) planes with good orientation estimates and (h)-(j) correctly classified non-planes.

REFERENCES

Bartoli, A. (2007). A random sampling strategy for piecewise planar scene segmentation. *Computer Vision and Image Understanding*, 105(1).

Birchfield, S. and Rangarajan, S. (2005). Spatiograms versus histograms for region-based tracking. In *Computer Vision and Pattern Recognitionn*, volume 2.

Choi, S. (2008). Algorithms for orthogonal nonnegative matrix factorization. In *International Joint Conference on Neural Networks*. IEEE.

Deerwester, S., Dumais, S., Furnas, G., Landauer, T., and Harshman, R. (1990). Indexing by latent semantic analysis. *Journal of the American society for Information Science*, 41(6).

Fergus, R., Perona, P., and Zisserman, A. (2005). A sparse object category model for efficient learning and exhaustive recognition. In *Computer Vision and Pattern Recognition*, volume 1.

Gee, A., Chekhlov, D., Calway, C., and Mayol-Cuevas, W. (2008). Discovering higher level structure in visual slam. *Transactions on Robotics*, 24.

Haines, O. and Calway, A. (2011). Estimating planar structure in single images by learning from examples. Technical Report CSTR-11-005, University of Bristol.

Hoiem, D., Efros, A., and Hebert, M. (2007). Recovering surface layout from an image. *International Journal of Computer Vision*, 75(1).

Košecká, J. and Zhang, W. (2005). Extraction, matching, and pose recovery based on dominant rectangular structures. *Computer Vision and Image Understanding*, 100(3).

Lowe, D. (2004). Distinctive image features from scale-invariant keypoints. *International Journal of Computer Vision*.

Martínez-Carranza, J. and Calway, A. (2010). Unifying planar and point mapping in monocular slam. In *British Machine Vision Conference*.

Michels, J., Saxena, A., and Ng, A. (2005). High speed obstacle avoidance using monocular vision and reinforcement learning. In *International Conference on Machine learning*.

Mičušík, B., Wildenauer, H., and Košecká, J. (2008). Detection and matching of rectilinear structures. In *Computer Vision and Pattern Recognition*.

Ó Conaire, C., O'Connor, N. E., and Smeaton, A. F. (2007). An improved spatiogram similarity measure for robust object localisation. In *International Conference on Acoustics, Speech and Signal Processing*, volume 1.

Rosten, E. and Drummond, T. (2006). Machine learning for high-speed corner detection. *Lecture Notes in Computer Science*, 3951.

Saxena, A., Sun, M., and Ng, A. (2008). Make3d: learning 3d scene structure from a single still image. *Transactions on Pattern Analysis and Machine Intelligence*.